Amroc - A Cartesian SAMR Framework for Compressible Gas Dynamics

Ralf Deiterding
Computer Science and Mathematics Division
Oak Ridge National Laboratory
Oak Ridge, Tennessee

SIAM Conference on Computational Science and Engineering
Costa Mesa, California
February 22, 2007

Collaboration with

- Sean Mauch and Daniel Meiron (Applied and Computational Mathematics Caltech)
- Fehmi Cirak (University of Cambridge)
- David Hill, Dale Pullin (Graduate Aeronautical Laboratories Caltech) and Carlos Pantano (University of Illinois at Urbana-Champaign)

This work is sponsored by the Office of Advanced Scientific Computing Research; U.S. Department of Energy (DOE) and was performed at the Oak Ridge National Laboratory, which is managed by UT-Battelle, LLC under Contract No. DE-AC05-00OR22725. Part of this work was also performed at the California Institute of Technology and was supported by the ASC program of the Department of Energy under subcontract No. B341492 of DOE contract W-7405-ENG-48.

Outline of the talk

- Computation of compressible flows in Amroc
  - *Currently supported equations and schemes*
- Dynamically adaptive Cartesian meshes
  - *Principles of hyperbolic SAMR, parallelization*
  - *Non-trivial examples*
- Incorporation of complex boundaries
  - *Level-set based ghost fluid approach*
  - *Verification and validation*
- Incorporation of Lagrangian solid mechanics solvers
  - *Fluid-structure coupling approach*
  - *Verification and validation*
  - *Multi-physics examples*
- Framework design and realization of complex methods
- Conclusions

Hydrodynamic equations

Favre-averaged Navier-Stokes equations

$$\frac{\partial \bar{\rho}}{\partial t} + \frac{\partial}{\partial x_k}(\bar{\rho}\tilde{u}_k) = 0$$

$$\frac{\partial}{\partial t}(\bar{\rho}\tilde{u}_i) + \frac{\partial}{\partial x_k}(\bar{\rho}\tilde{u}_i\tilde{u}_k + \delta_{ik}\bar{p} - \tilde{\tau}_{ik} + \sigma_{ik}) = 0$$

$$\frac{\partial \bar{E}}{\partial t} + \frac{\partial}{\partial x_k}(\tilde{u}_k(\bar{E} + \bar{p}) + \tilde{q}_k - \tilde{\tau}_{kj}\tilde{u}_j + \sigma_k^e) = 0$$

$$\frac{\partial}{\partial t}(\bar{\rho}\tilde{Y}_i) + \frac{\partial}{\partial x_k}(\bar{\rho}\tilde{Y}_i\tilde{u}_k + \tilde{J}_k^i + \sigma_k^i) = \dot{m}_i$$

Implicit equation of state

$$\bar{\rho}\tilde{h} - \bar{p} - \bar{E} + \frac{1}{2}\bar{\rho}\tilde{u}_k\tilde{u}_k + \bar{\rho}k_{sgs} = 0$$

Ideal gas law

$$\bar{p} = \bar{\rho}\mathcal{R}(\tilde{T}\sum_{i=1}^{N}\frac{\tilde{Y}_i}{W_i} + w_s)$$

Caloric equation

$$\tilde{h} = \sum_{i=1}^{N} h_i(\tilde{T})\tilde{Y}_i + h_s \quad \text{with}$$

$$h_i(\tilde{T}) = h_i^o + \int_{T_0}^{\tilde{T}} c_{pi}(T^*)dT^*$$

Stress tensor and diffusion terms

$$\tilde{\tau}_{ik} = \tilde{\mu}\left(\frac{\partial \tilde{u}_k}{\partial x_i} + \frac{\partial \tilde{u}_i}{\partial x_k}\right) - \frac{2}{3}\tilde{\mu}\frac{\partial \tilde{u}_j}{\partial x_j}\delta_{ik}$$

$$\tilde{q}_k = -\tilde{\lambda}\frac{\partial \tilde{T}}{\partial x_k} \qquad \tilde{J}_k^i = -\bar{\rho}\tilde{D}_i\frac{\partial \tilde{Y}_i}{\partial x_k}$$

Chemical kinetics with Arrhenius law

$$\dot{m}_i = W_i\sum_{j=1}^{M}(\nu_{ji}^r - \nu_{ji}^f)[k_j^f\prod_{n=1}^{N}\left(\frac{\rho_n}{W_n}\right)^{\nu_{jn}^f} - k_j^r\prod_{n=1}^{N}\left(\frac{\rho_n}{W_n}\right)^{\nu_{jn}^r}]$$

Simulation of compressible flows

- Convective part
  - *Conservative schemes with upwinding in all characteristic fields*
  - *Time-explicit treatment with Riemann solvers*
  - *Centered schemes in smooth solutions regions possible*
  - *Shock waves can not be resolved in practice* $\rightarrow$ *weak solutions of Euler equations are sought*
  - *Unique solution is determined by entropy condition*
- Diffusion terms
  - *Conservative centered differences*
- Source terms
  - *Fractional splitting method, typically with explicit or semi-implicit Runge-Kutta ODE schemes with automatic stepsize adjustment*
  - *With non-linear source terms the wave speeds become resolution-dependent, even with finite volume methods* $\rightarrow$ *very high local resolution necessary*

- Schemes are implemented in single grid routines, typically in F77/F90
  - *Clawpack version with extended higher-order capabilities and large number of Riemann solvers*
  - *Hydrid WENO-TCD method by D. Hill and C. Pantano with LES model for compressible flows by D. Pullin*
  - *Riemann Invariant Manifold Method by T. Lappas*
  - *Finite volume MHD solver by M. Torrilhon (only uniform for now)*

Structured AMR for hyperbolic problems

- For simplicity

$$\partial_t \mathbf{q} + \nabla \cdot \mathbf{f}(\mathbf{q}) = 0$$

- Refined subgrids overlay coarser ones
- Computational decoupling of subgrids by using ghost cells
- Refinement in space *and* time
- Block-based data structures
- Cells without mark are refined
- Cluster-algorithm necessary
- Efficient cache-reuse / vectorization possible
- Explicit finite volume scheme

$$\mathbf{Q}^{n+1}_{jk} = \mathbf{Q}^{n}_{jk} - \frac{\Delta t}{\Delta x_1}\left[\mathbf{F}^1_{j+\frac{1}{2},k} - \mathbf{F}^1_{j-\frac{1}{2},k}\right] - \frac{\Delta t}{\Delta x_2}\left[\mathbf{F}^2_{j,k+\frac{1}{2}} - \mathbf{F}^2_{j,k-\frac{1}{2}}\right]$$

only for single rectangular grid necessary

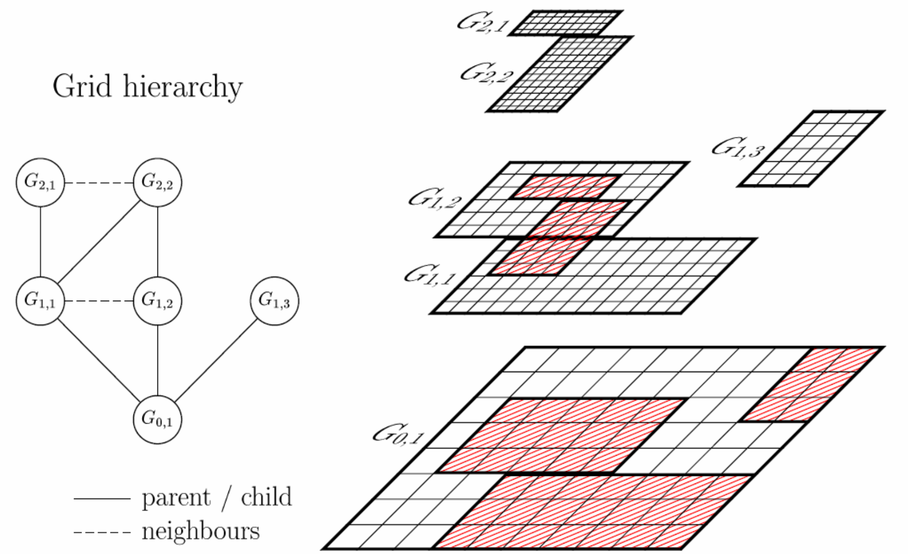

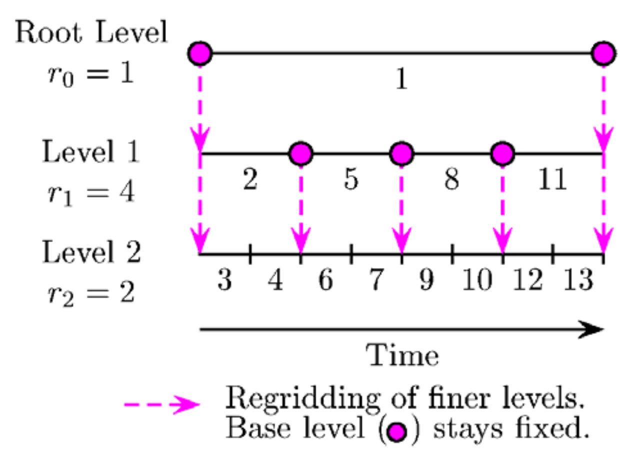

Parallelization strategy

Domain decomposition: $G_0 = \bigcup_{p=1}^{P} G_0^p$ with $G_0^p \cap G_0^q = \emptyset$ for $p \neq q$

$$G_0^p := \bigcup_{m=1}^{M_0^p} G_{0,m}^p \quad \longrightarrow \quad G_l^p := G_l \cap G_0^p$$

Workload: $\mathcal{W}(\Omega) = \sum_{l=0}^{l_{\max}} \left[\mathcal{N}_l(G_l \cap \Omega) \prod_{\kappa=0}^{l} r_\kappa \right]$, $\mathcal{N}_l(G)$ No. of cells on l

Load-balacing: $\mathcal{L}^p := \dfrac{P \cdot \mathcal{W}(G_0^p)}{\mathcal{W}(G_0)} \approx 1$ for all $p = 1, \ldots, P$

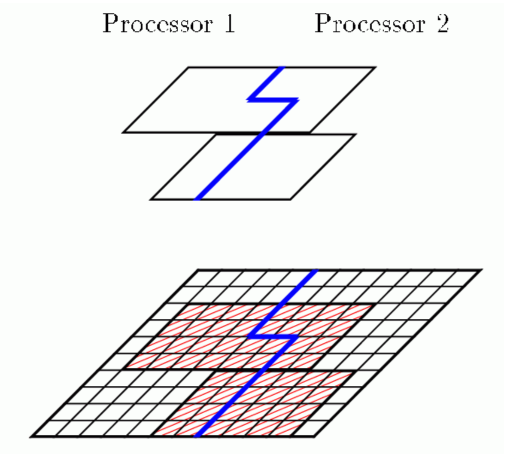

- Data of all levels resides on same node $\rightarrow$ Interpolation and averaging remain strictly local
- Only parallel operations to be considered:
  - *Parallel synchronization as part of ghost cell setting*
  - *Load-balanced repartitioning of data blocks as part of* **`Regrid(l)`**
  - *Application of flux correction terms on coarse-grid cells*
- Partitioning at root level with generalized Hilbert space-filling curve by M. Parashar

UML design of Amroc

- Classical framework approach with generic main program in C++
- Customization / modification in Problem.h include file by derivation from base classes and redefining virtual interface functions
- Predefined, scheme-specific classes (with F77 interfaces) provided for standard simulations
- Standard simulations require only linking to F77 functions for initial and boundary conditions, source terms. No C++ knowledge required.
- Interface mimics Clawpack
- Expert usage (algorithm modification, advanced output, etc.) in C++

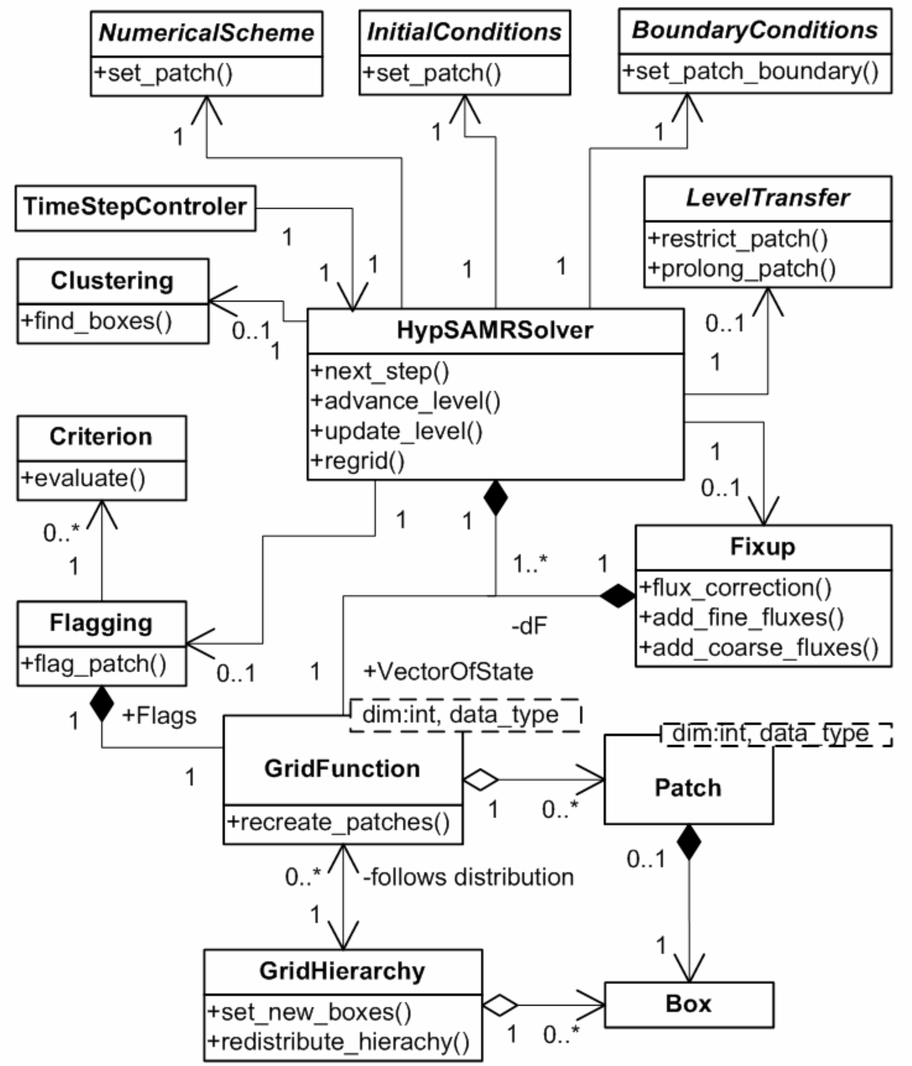

Planar Richtmyer-Meshkov Instability

- Treat turbulent region in flow as a ‘feature’ to be refined
  - *Containment of turbulence in refined zones*
  - *Turbulent base level resolution used as subgrid cutoff*
- Perturbed Air-SF6 interface shocked and re-shocked by Mach 1.5 shock
- 96 CPUs IBM SP2-Power3 by D. Hill, C. Pantano
- WENO-TCD by D. Hill scheme with LES model by D. Pullin for Favre-averaged Navier-Stokes equations
  - *AMR base grid 172x56x56, 2 additional levels with factors 2, 2*
  - *$9 \cdot 10^6$ cells in average instead of $34 \cdot 10^6$ (uniform)*
- Mixing width agrees with experimental results by Vetter, Sturtevant (1995)

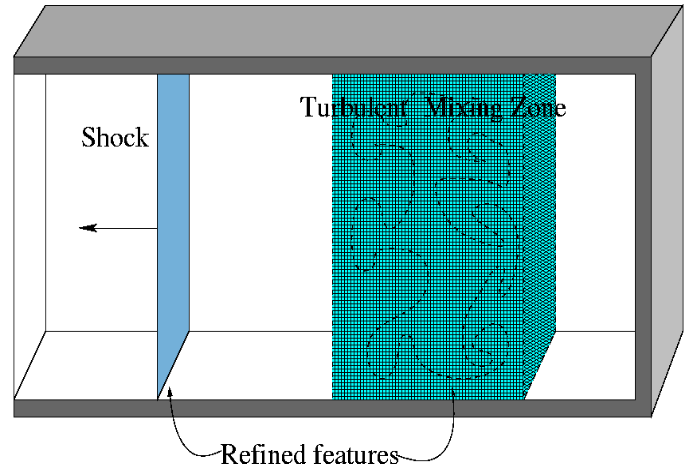

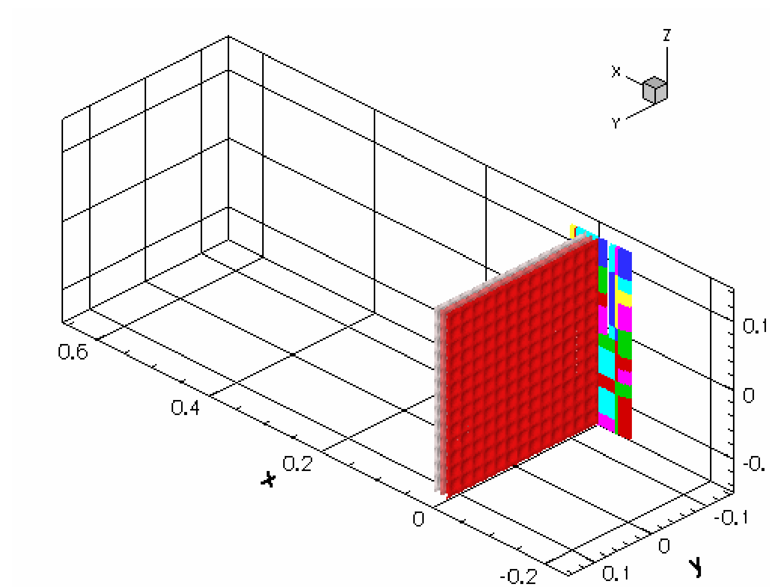

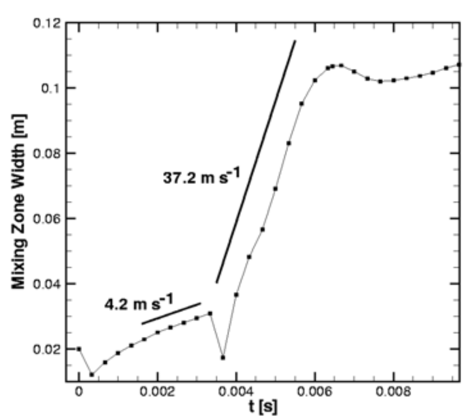

Ghost fluid method

- Incorporate complex moving boundary/ interfaces into a Cartesian solver (extension of work by R. Fedkiw and T. Aslam)
- Implicit boundary representation via distance function φ, normal $n = \nabla\varphi / |\nabla\varphi|$
- Treat an interface as a moving rigid wall
- Method diffuses boundary and is therefore not conservative
- Construction of values in embedded boundary cells by interpolation / extrapolation

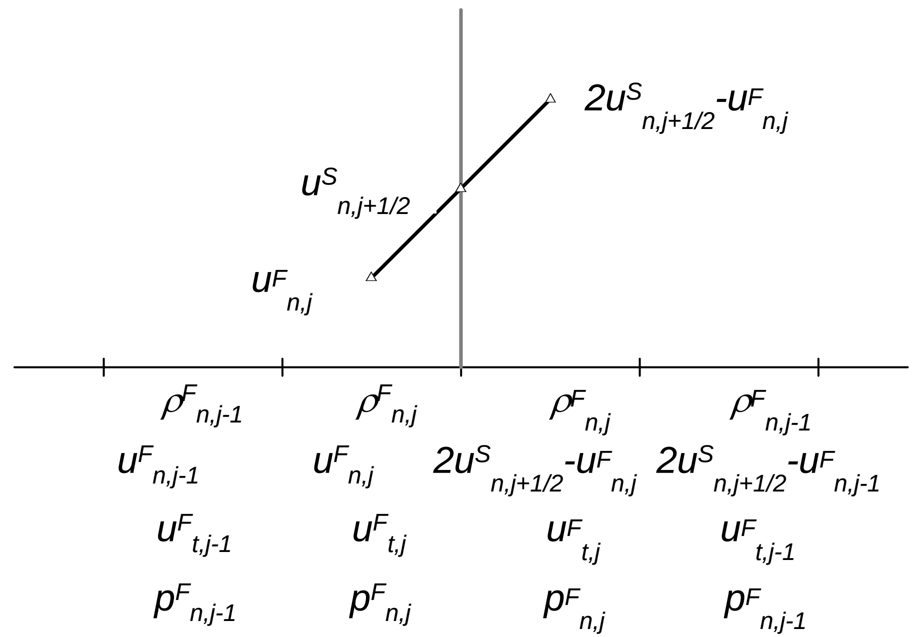

Velocity: $\mathbf{u}^F_{Gh} = 2((\mathbf{u}^S - \mathbf{u}^F_M)\cdot\mathbf{n})\,\mathbf{n} + \mathbf{u}^F_M$

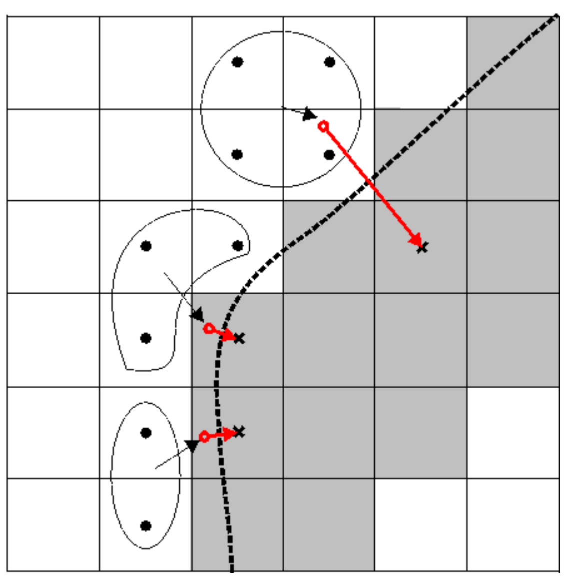

- Higher resolution at embedded boundary usually required than with first-order unstructured scheme
- Appropriate level-set-based refinement criteria are available

Ghost fluid method in Amroc

- Core algorithm implemented in derived HypSAMRSolver class
- Multiple independent EmbeddedBoundaryMethod objects possible
- Base classes are scheme-independent
- Specialization of GFM boundary conditions, level set description in scheme-specific F77 interface classes

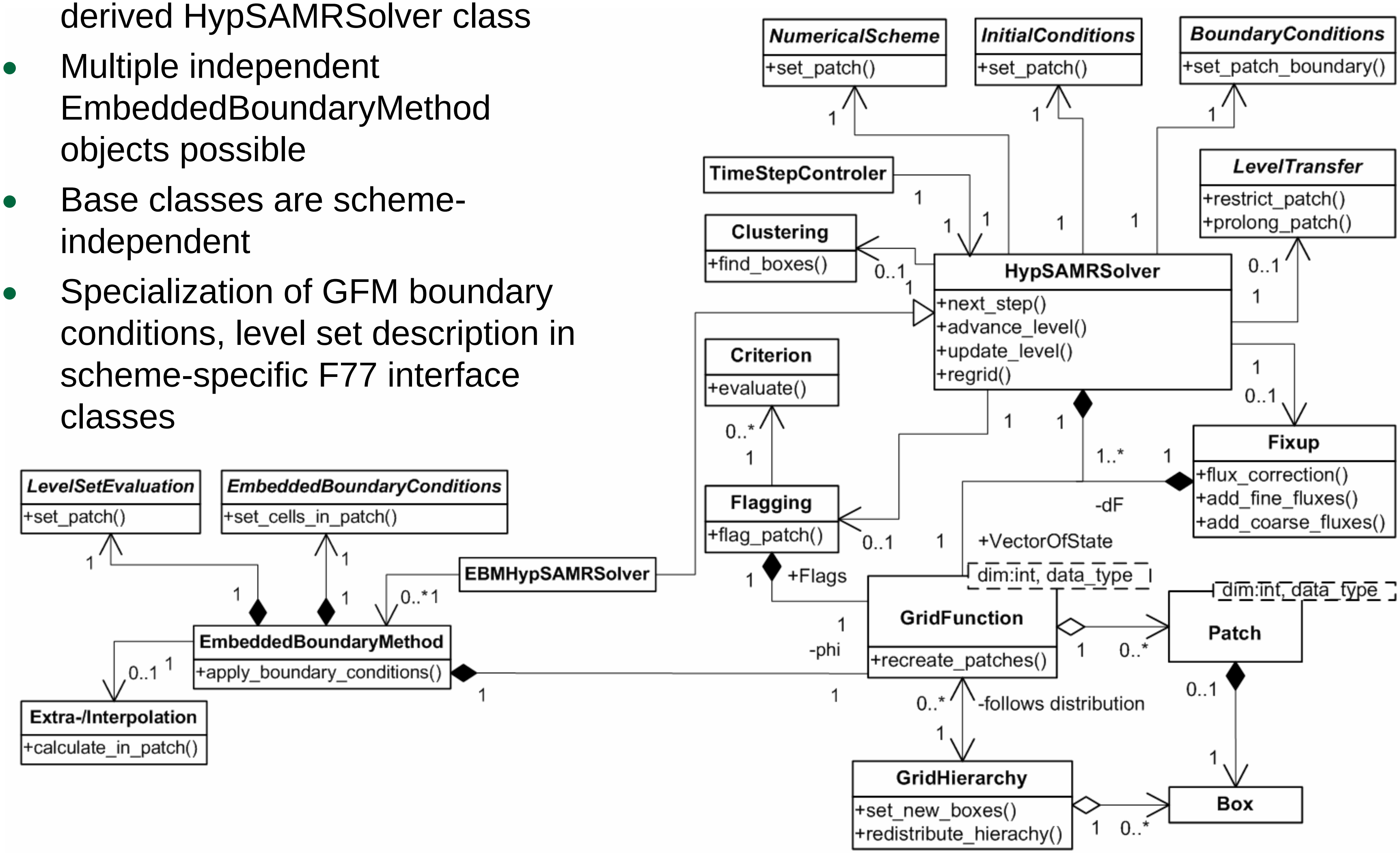

Verification of GFM

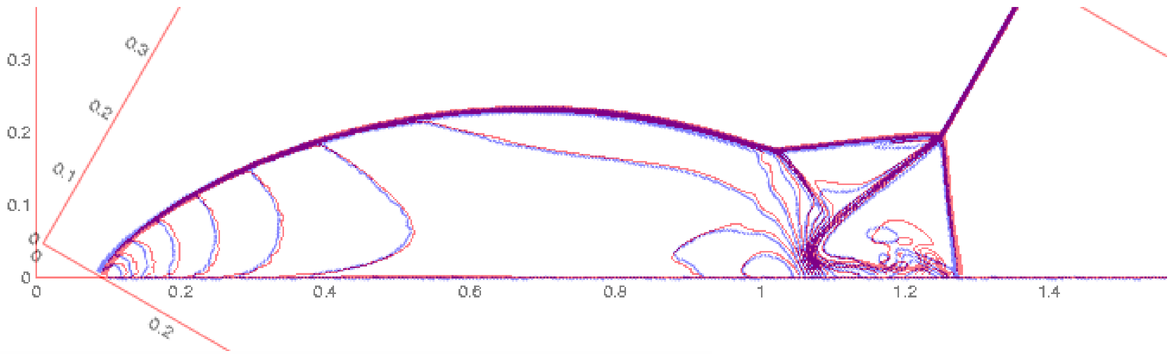

Double Mach reflection

Overlay of two simulation of a double Mach reflection on a 800x400 grid with GFM and 2nd order accurate scheme

Conical shocktube

Cylindrical symmetric simulation by D. Hill of experiment by Setchel, Strom and Sturtevant (JFM 1972)

Mach 6 shock in Argon

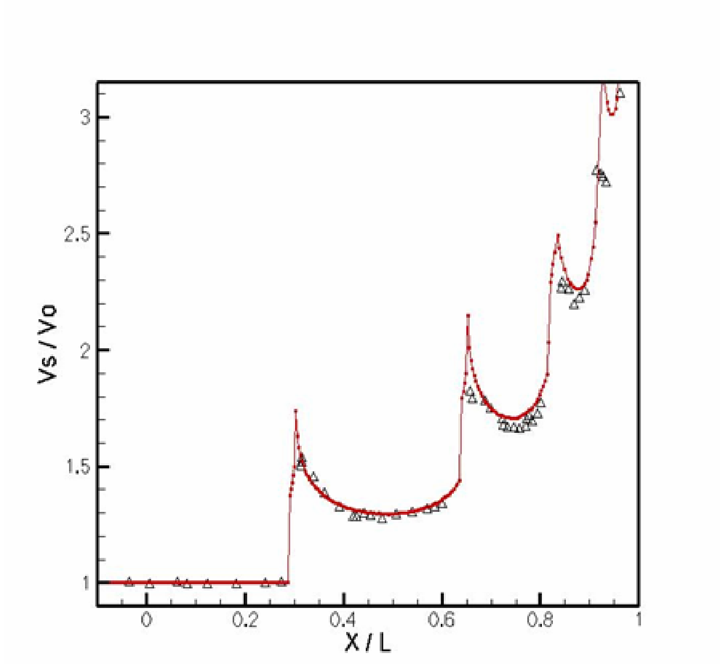

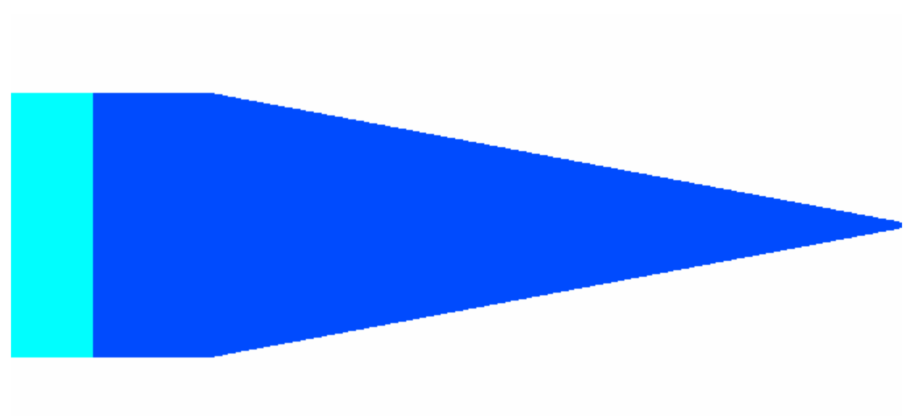

Left: shock velocity along centerline in experiment and simulation (red)

Shock interaction at double-wedge geometry

- Simulation by D. Hill
- Mach 9 flow in air hitting a double-wedge (15^o and 45^o)
- Example from Olejniczak, Wright and Candler (JFM 1997)
- AMR base mesh 300x100, 3 additional levels with factor 2
- 3^{rd} order WENO computation vs. 2^{nd} order MUSCL with van Leer flux vector splitting

10 *J. Olejniczak, M. J. Wright and G. V. Candler*

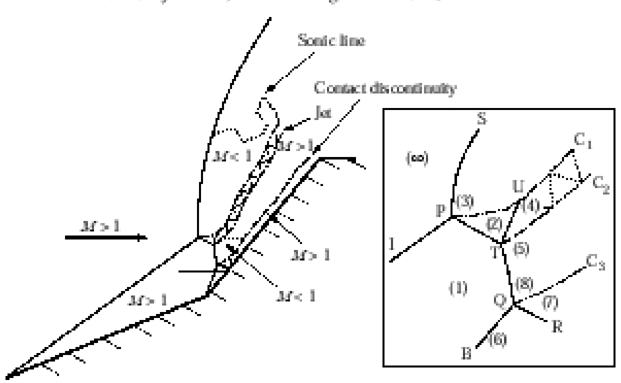

FIGURE 6. Schematic diagram of a Type V shock interaction with an enlargement of the interaction region.

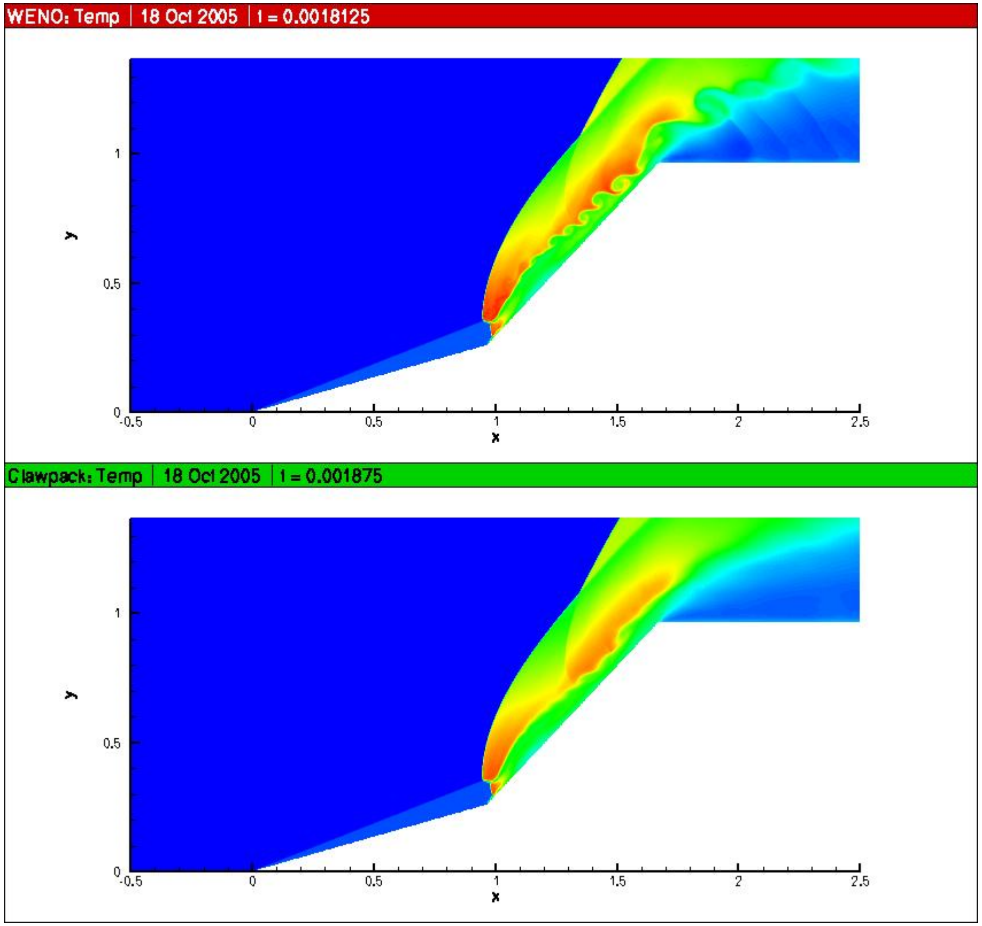

Fluid-structure coupling

- Couple compressible Euler equations to Lagrangian structure mechanics
- Compatibility conditions between inviscid fluid and solid at a slip interface
  - *Continuity of normal velocity: $u^S_n = u^F_n$*
  - *Continuity of normal stresses: $\sigma^S_{nn} = -p^F$*
  - *No shear stresses: $\sigma^S_{n\tau} = \sigma^S_{n\omega} = 0$*

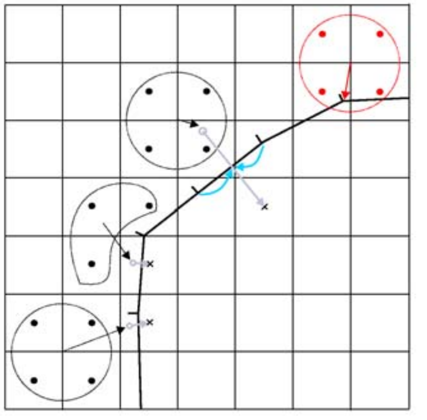

- Time-splitting approach for coupling
  - *Fluid:*
    - *Treat evolving solid surface with moving wall boundary conditions in fluid*
    - *Use solid surface mesh to calculate fluid level set*
    - *Use nearest velocity values $\mathbf{u}^S$ on surface facets to impose u^F_n in fluid*
  - *Solid:*
    - *Use interpolated hydro-pressure p^F to prescribe σ^S_{nn} on boundary facets*
- Ad-hoc separation in dedicated fluid and solid processors

Algorithmic approach for coupling

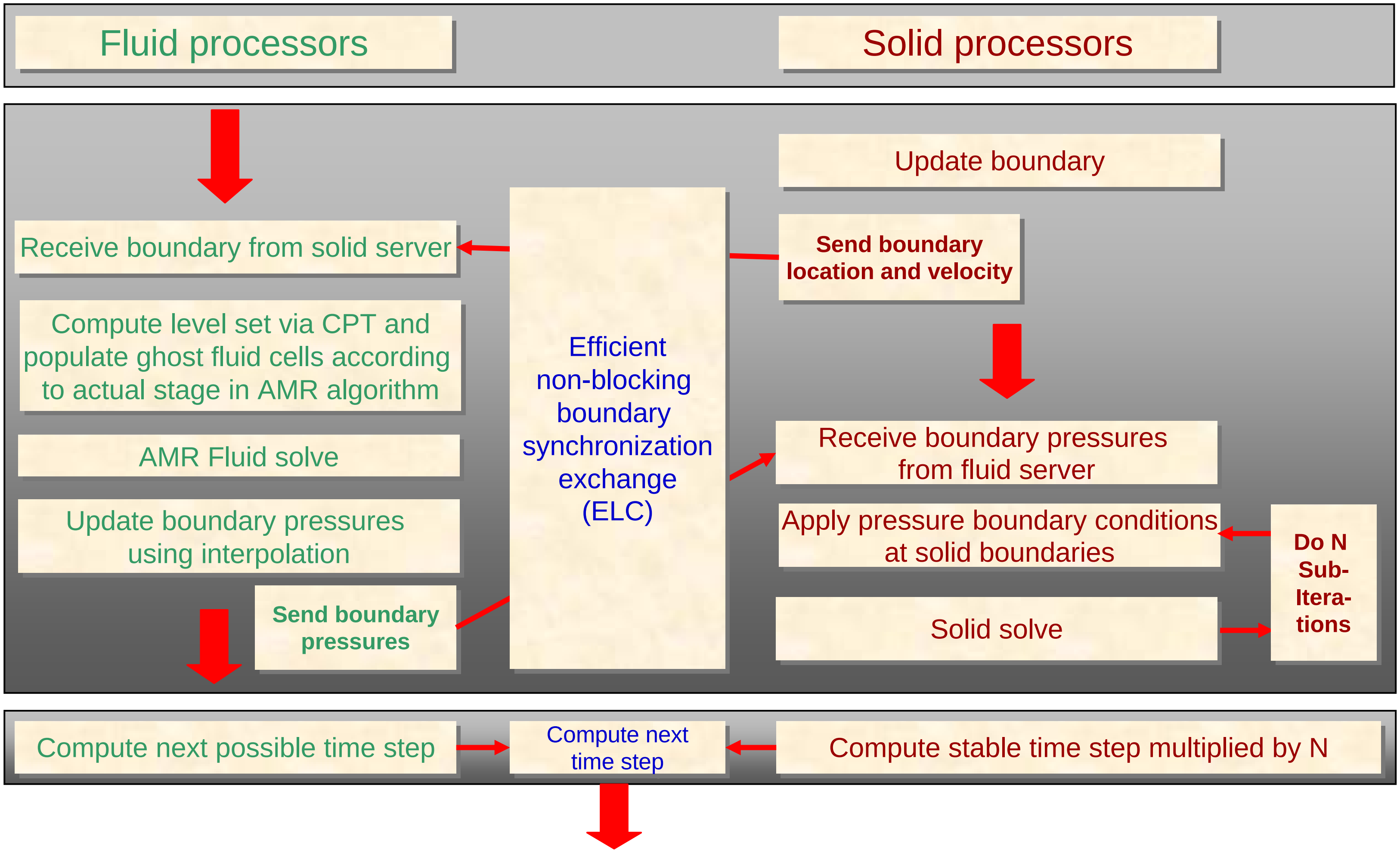

Implicit representations of complex surfaces

- FEM Solid Solver
  - *Explicit representation of the solid boundary, b-rep*
  - *Triangular faceted surface*
- Cartesian FV Solver
  - *Implicit level set representation*
  - *need closest point on the surface at each grid point*

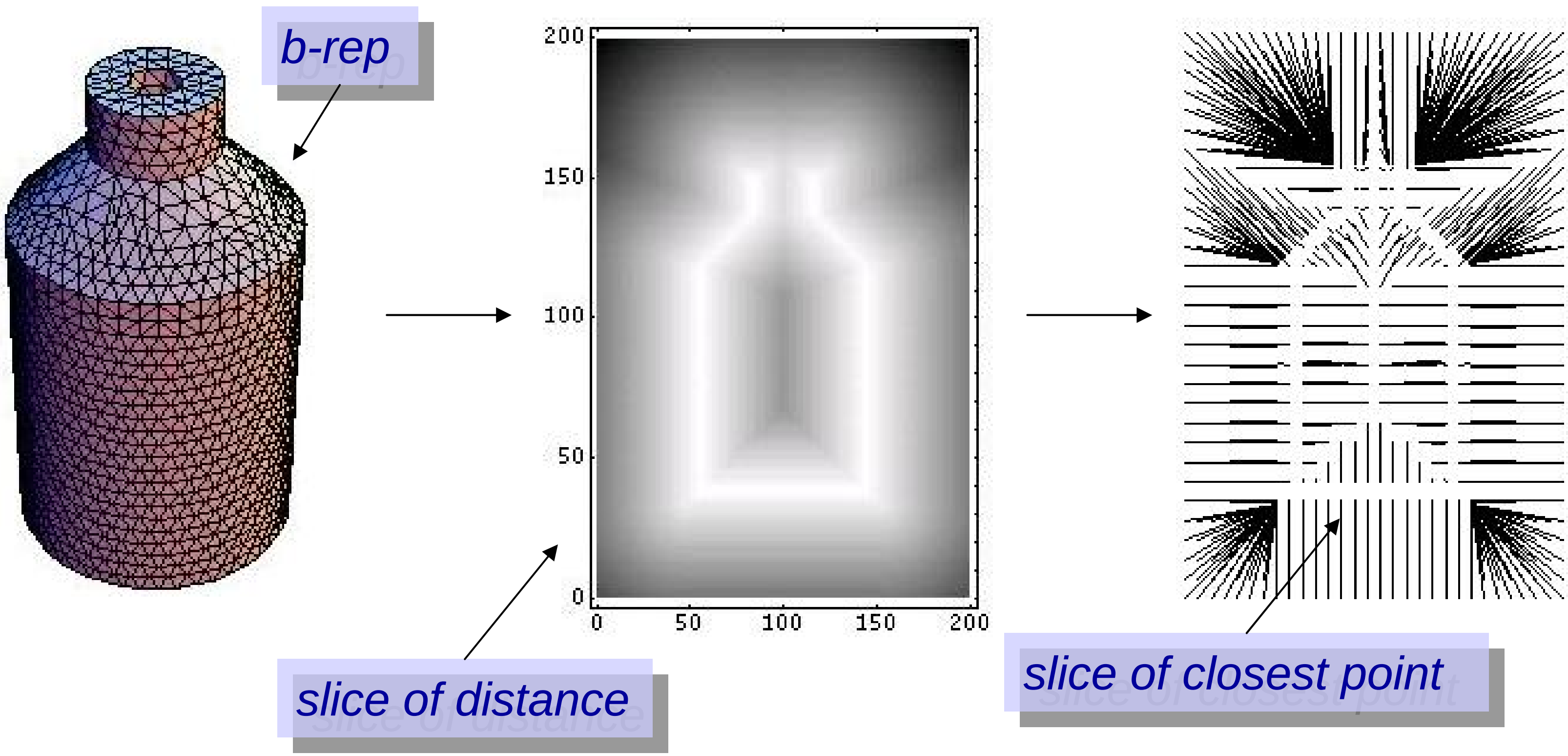

→ Closest point transform algorithm (CPT) by S. Mauch

Amroc coupled to CSD solver (the VTF)

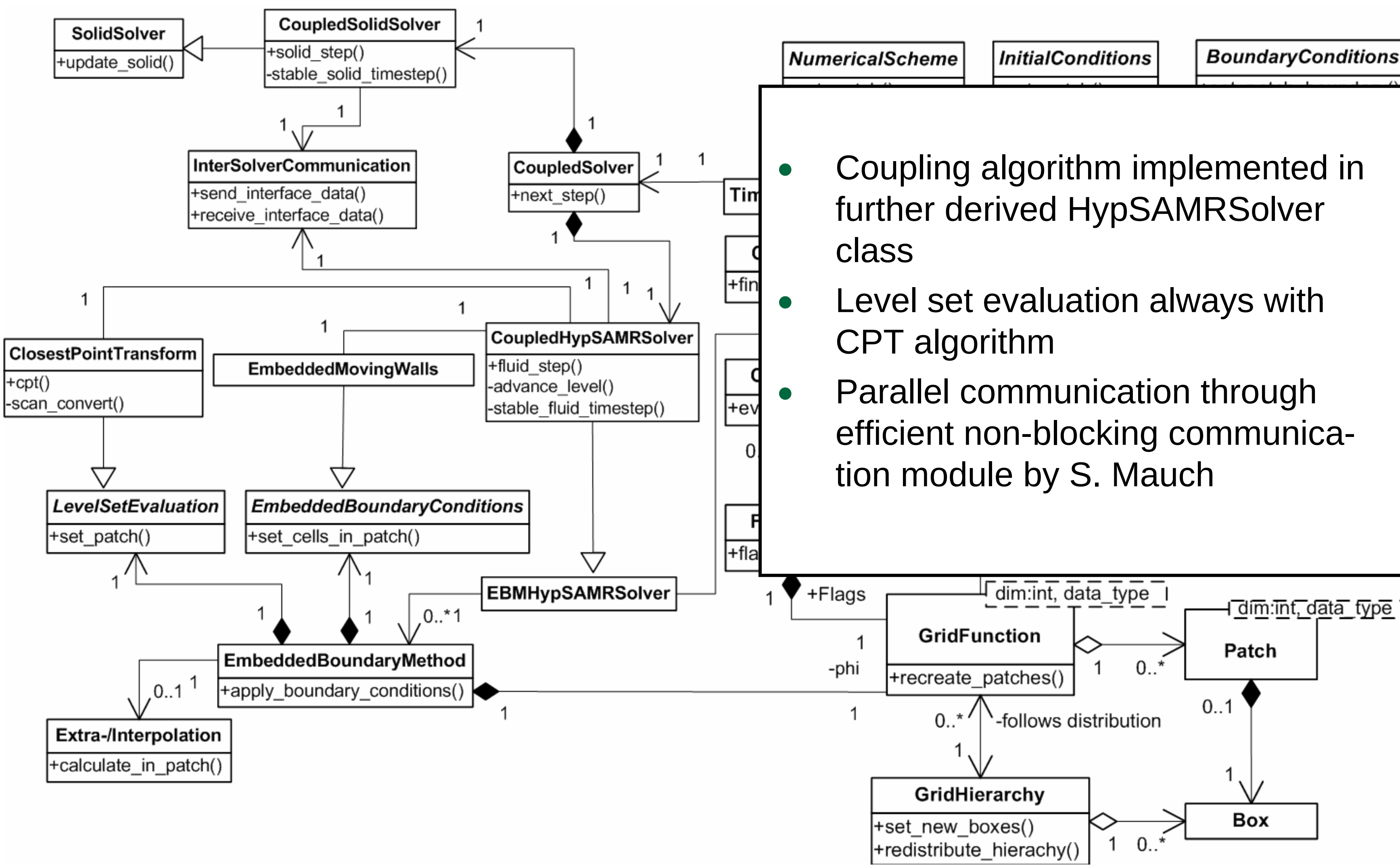

- Coupling algorithm implemented in further derived HypSAMRSolver class
- Level set evaluation always with CPT algorithm
- Parallel communication through efficient non-blocking communication module by S. Mauch

- Elastic motion of a thin steel plate when being hit by a Mach 1.21 shock wave, Giordano et al. Shock Waves (2005)
- Steel plate modeled with finite difference solver using the beam equation

$$\rho h \frac{\partial^2 w}{\partial t^2} + EI \frac{\partial^4 w}{\partial x^4} = p(x,t)$$

- SAMR base mesh 320x64, 2 additional level with factors 2, 4

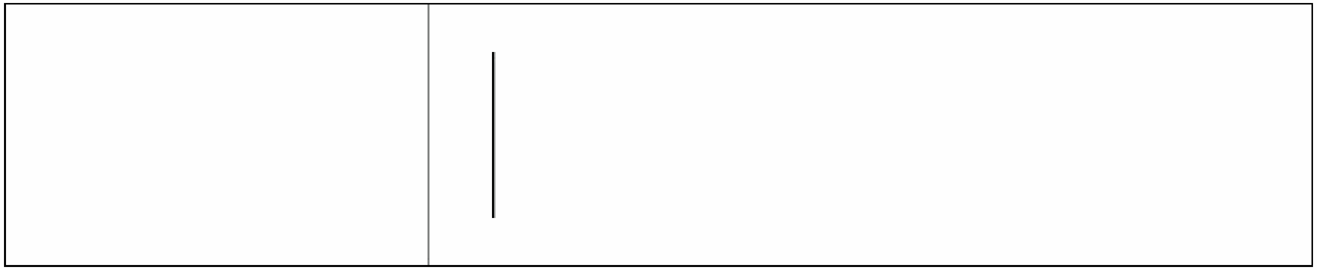

Schlieren plot of density

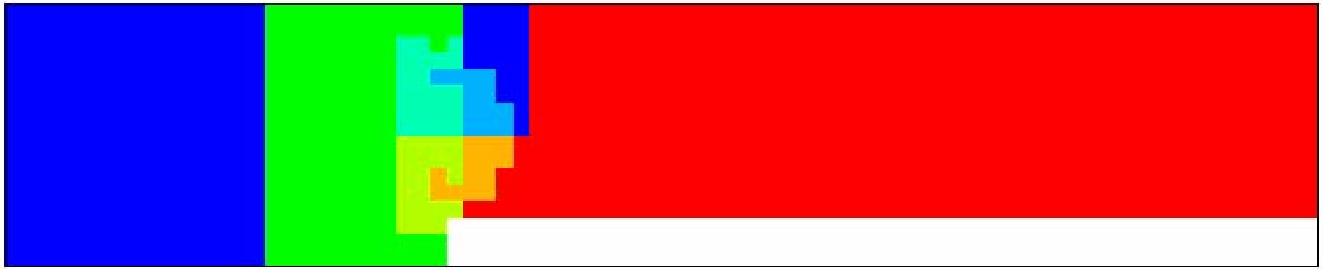

Distribution to 7 fluid processors

- Elastic motion of a thin steel plate when being hit by a Mach 1.21 shock wave, Giordano et al. Shock Waves (2005)
- Steel plate modeled with finite difference solver using the beam equation

$$\rho h \frac{\partial^2 w}{\partial t^2} + EI \frac{\partial^4 w}{\partial x^4} = p(x,t)$$

- SAMR base mesh 320x64, 2 additional level with factors 2, 4

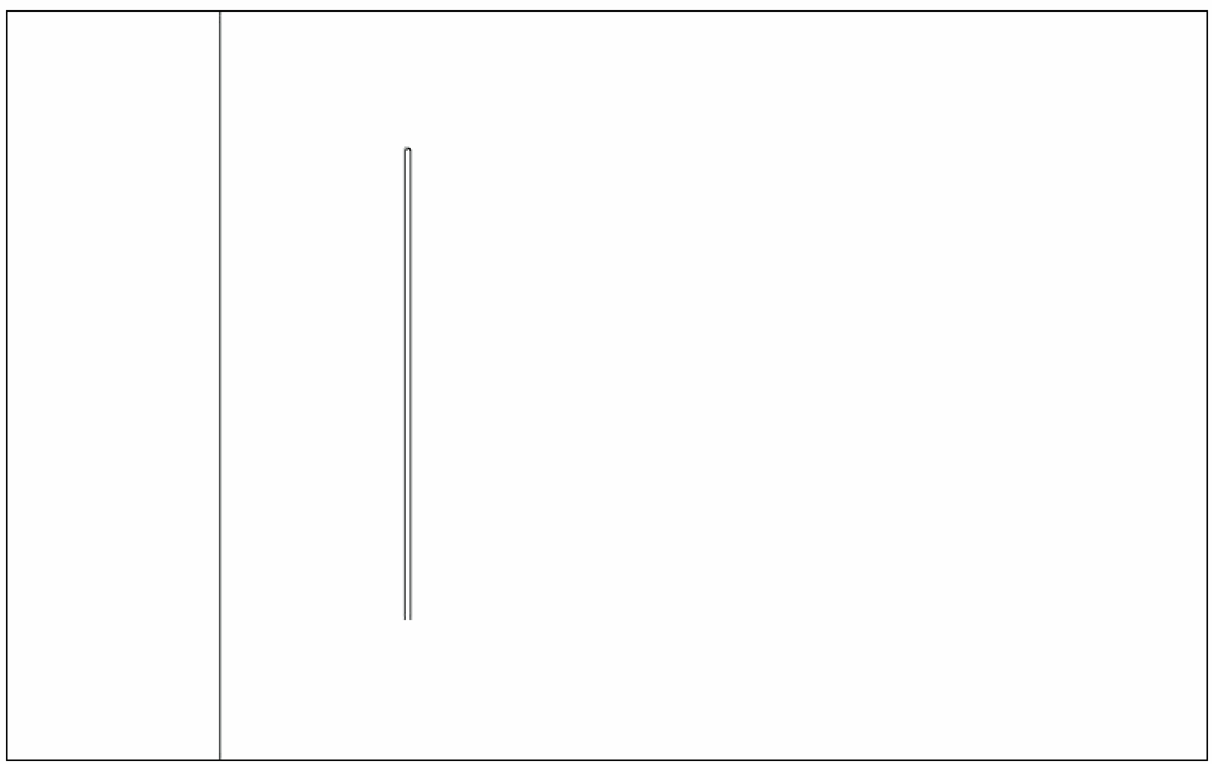

Schlieren plot of density

Validation example: detonation-driven fracture

- Experiments by T. Chao, J. C. Krok, J. Karnesky, F. Pintgen, J.E. Shepherd (GalCIT)
- Motivation: Validate VTF for complex fluid-structure interaction problem
- Interaction of detonation, ductile deformation, fracture
- Modeling of ethylene-oxygen detonation with constant volume burn detonation model

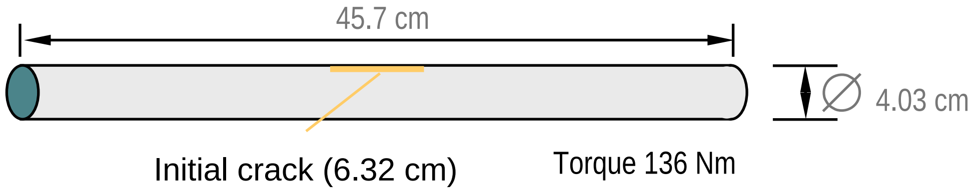

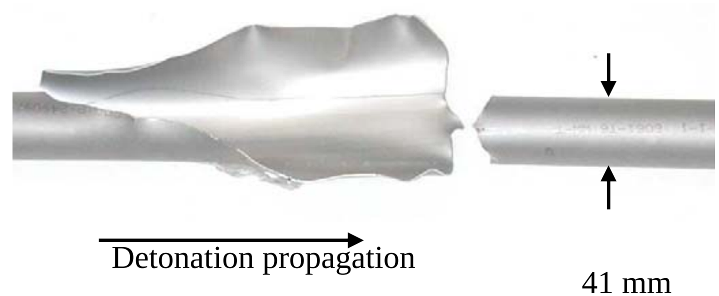

Treatment of shells/thin structures

- Thin boundary structures or lower-dimensional shells require “thickening” to apply ghost fluid method
  - *Unsigned distance level set function* φ
  - *Treat cells with* $0<\varphi<d$ *as ghost fluid cells (indicated by green dots)*
  - *Leaving* φ *unmodified ensures correctness of* $\nabla\varphi$
  - *Refinement criterion based on* φ *ensures reliable mesh adaptation*
  - *Use face normal in shell element to evaluate in* $\Delta p = p_u - p_l$

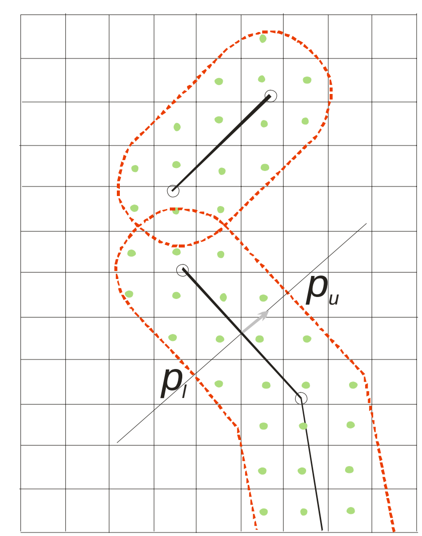

Fluid-structure interaction validation – tube with flaps

- $C_2H_4+3\,O_2$ CJ detonation for p_0=100 kPa drives plastic opening of pre-cut flaps
- Motivation:
  - *Validate fluid-structure interaction method*
  - *Validate material model in plastic regime*

Fluid

- Constant volume burn model
- AMR base level: 104x80x242, 3 additional levels, factors 2,2,4
- Approx. $4\cdot10^7$ cells instead of $7.9\cdot10^9$ cells (uniform)
- Tube and detonation fully refined
- Thickening of 2d mesh: 0.81 mm on both sides (real thickness on both sides 0.445 mm)

Solid

- Aluminum, J2 plasticity with hardening, rate sensitivity, and thermal softening
- Mesh: 8577 nodes, 17056 elements
- 16+2 nodes 2.2 GHz AMD Opteron quad processor, PCI-X 4x Infiniband network
- Ca. 4320h CPU to t=450 μs

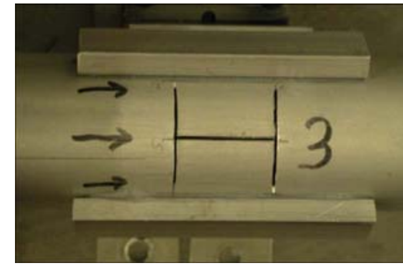

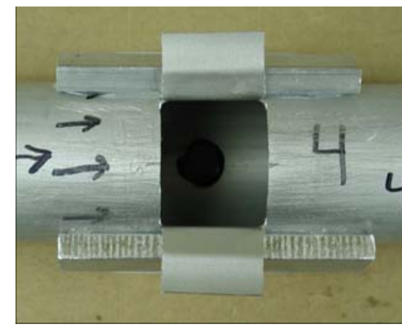

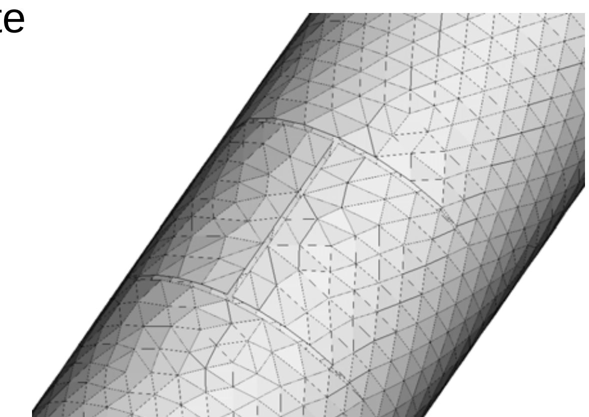

Tube with flaps – computational results

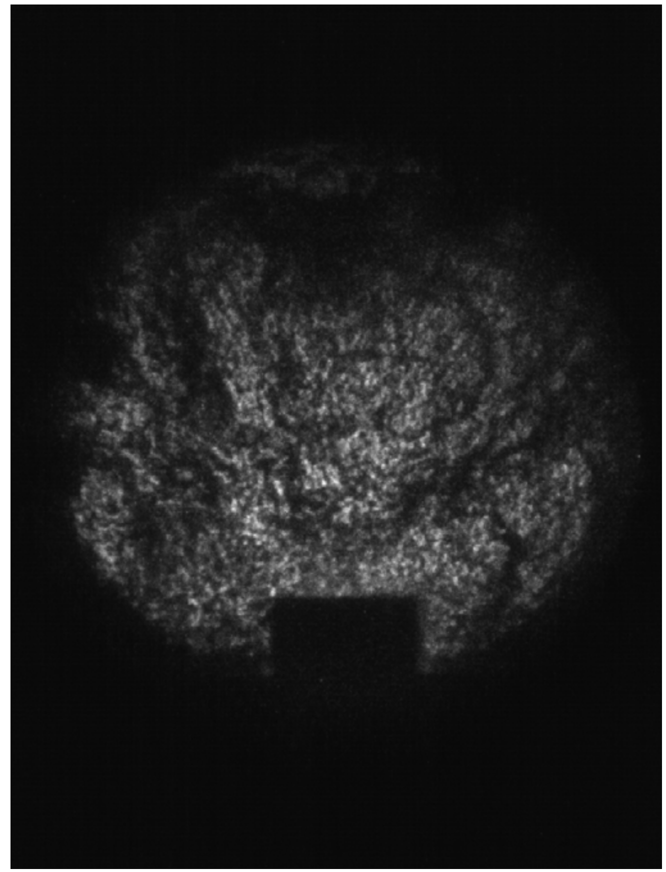

Simulated results at t=212 μs   Experimental results at t=210 μs

Tube with flaps - Results

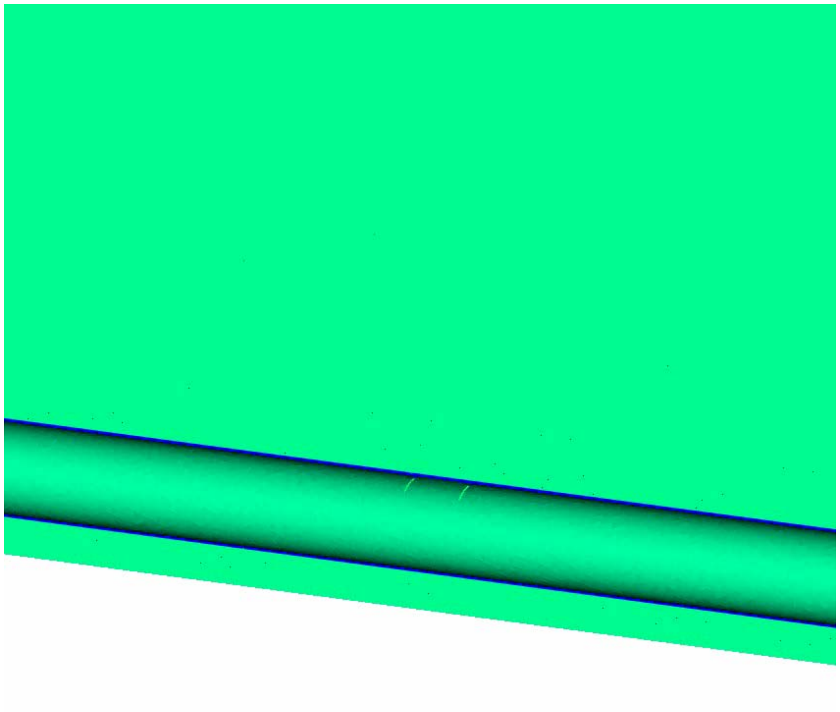

Fluid density and diplacement in y-direction in solid

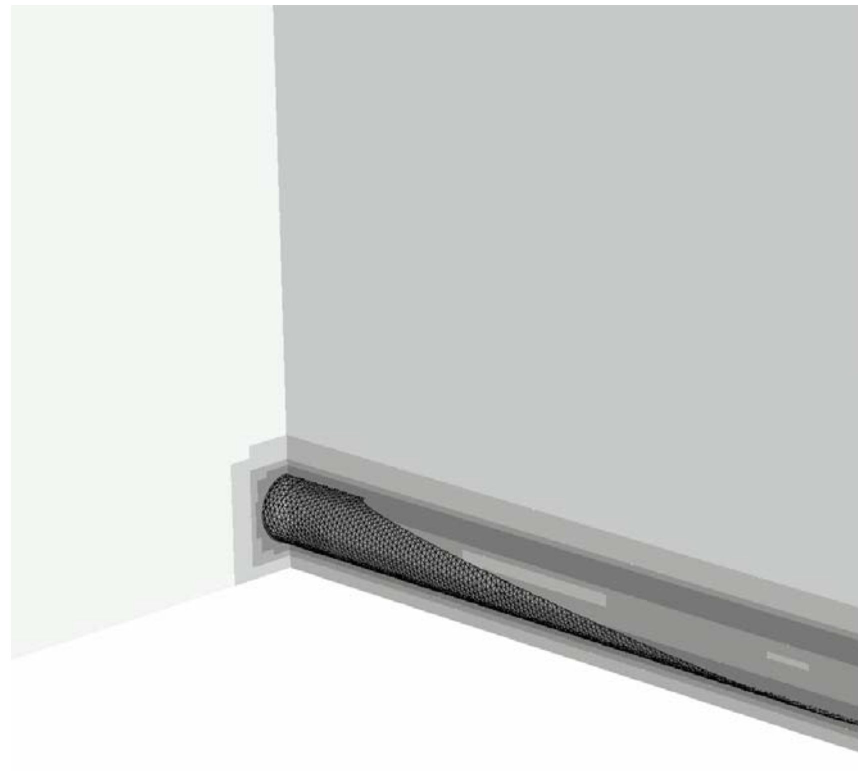

Schlieren plot of fluid density on refinement levels

Plate deformation from water hammer

- 3d simulation of plastic deformation of thin copper plate attached to the end of a pipe due to water hammer
- Strong over-pressure wave in water is induced by rapid piston motion at end of tube
- Simulation by R. Deiterding, F. Cirak. Experiment by V.S. Deshpande et al. (U Cambridge)

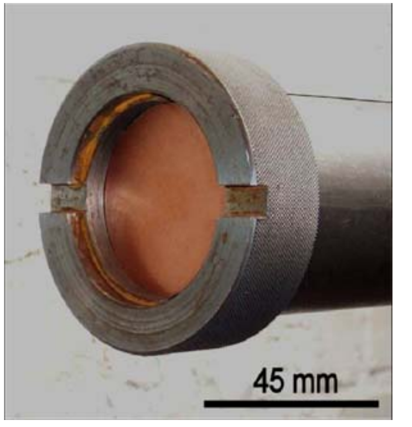

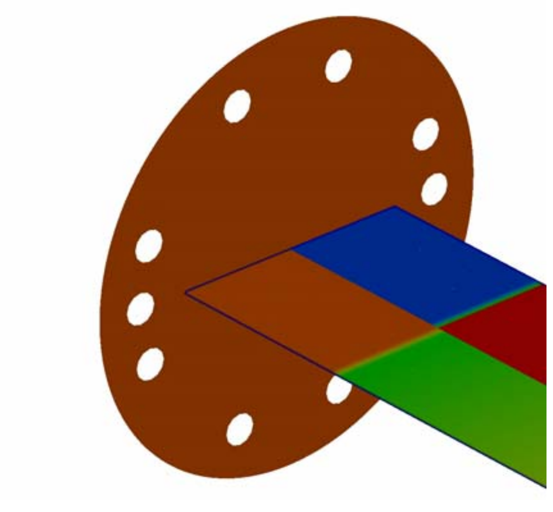

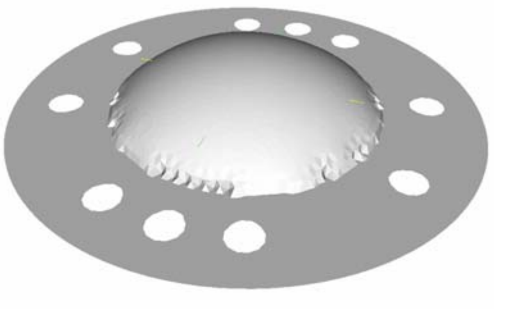

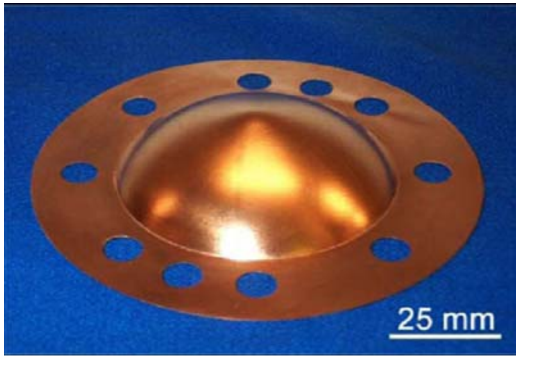

Comparison of plate at end of simulation and experiment (middle and right). Left: Color of plate and lower half of plane shows the normal velocity.

Simulation details

Fluid

- Pressure wave generated by solving equation of motion for piston during fluid-structure simulation
- Modeling of water with stiffened gas equation of state

$$p = (\gamma - 1)(E - \frac{1}{2} u_k u_k) - \gamma p_\infty$$

with γ=7.415, p_∞=296.2 MPa

- Multi-dimensional 2nd order upwind finite volume scheme, negative pressures from cavitation eliminated by energy correction
- AMR base level: 350x20x20, 2 additional levels, refinement factor 2,2
- Approx. $1.2 \cdot 10^6$ cells used in fluid on average instead of $9 \cdot 10^6$ (uniform)

Solid

- Copper plate of 0.25 mm, J2 plasticity model with hardening, rate sensitivity, and thermal softening
- Solid mesh: 4675 nodes, 8896 elements
- 8 nodes 3.4 GHz Intel Xeon dual processor, Gigabit ethernet network, ca. 130h CPU

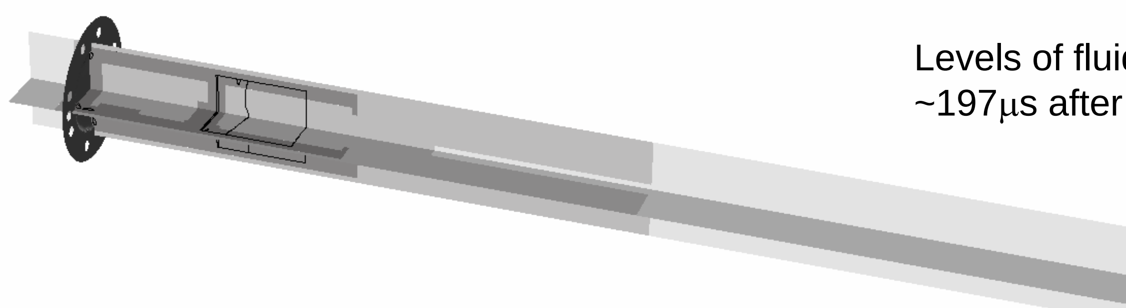

Levels of fluid mesh refinement (gray) ~197μs after wave impact onto plate.

Multi-physics examples with fracture

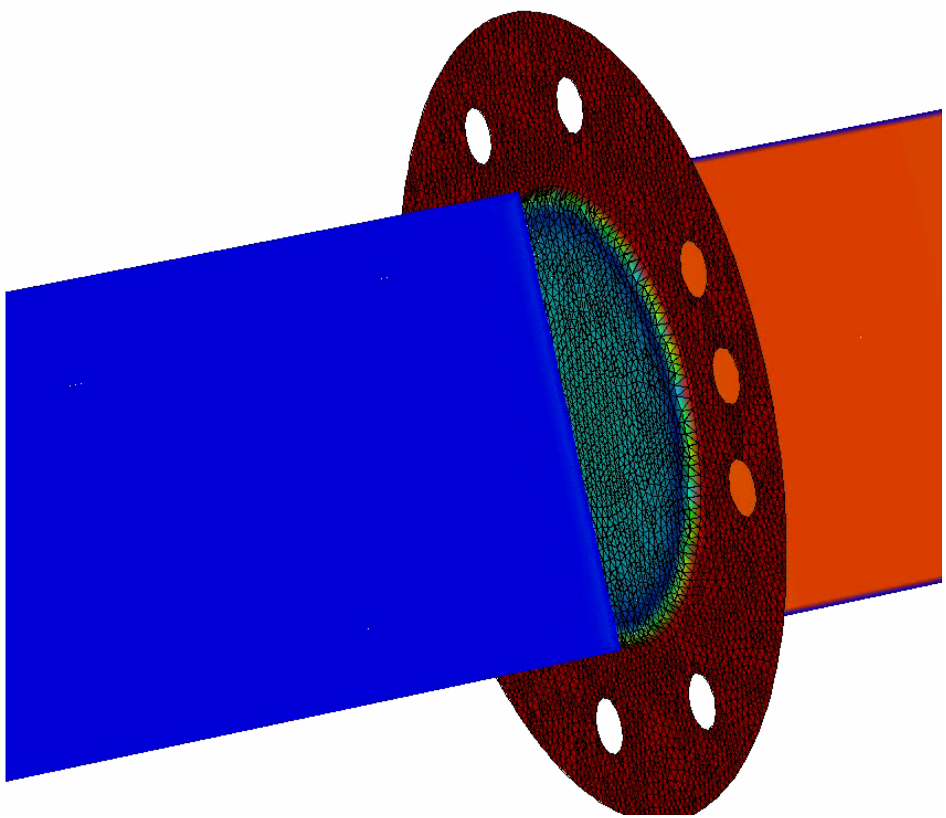

- *Copper plate fracture demo simulation*
- *Two-component solver with stiffened gas EOS for water and ideal gas EOS for air*
- *4+4 nodes 3.4 GHz Intel Xeon dual processor, ca. 550h CPU*

Conclusions

- Amroc: general object-oriented framework for implementing Cartesian methods
- Applications shown for compressible flows, but any hyperbolic system can easily be considered (software can directly use Riemann solvers from Clawpack by R. LeVeque)
  - *Advection*
  - *Acoustics*
  - *Shallow water*
  - *Elastic waves*
  - *Ideal magneto-hydrodynamics*
- Generic ghost fluid implementation allows consideration of (possible moving) embedded boundaries
- Boundaries can be described directly through level set functions or arbitrary triangulated surface meshes
- $\rightarrow$ any Cartesian finite volume scheme can be used for real-world computations, mesh adaptivity provides necessary accuracy increase
- Fluid-structure interaction coupling routines available to incorporate solid mechanics solvers, e.g. coupling to serial LLNL Dyna3d recently completed by J. Cummings, P. Hung (Caltech)
- Most recent Amroc within VTF: *http://www.cacr.caltech.edu/asc*

Abbreviations

- Amroc: Adaptive mesh refinement in object-oriented C++
- GFM: Ghost fluid method
- CPT: Closest point transform
- CSD: Computational solid dynamics
- FEM: Finite element
- FV: Finite volume
- JFM: Journal of fluid mechanics
- MUSCL: Monotone upstream-centered schemes for conservation laws
- MHD: Magneto-hydrodynamics
- ODE: Ordinary differential equations
- SAMR: Structured adaptive mesh refinement
- TCD: Tuned central difference
- UML: Unified modeling language
- VTF: Virtual Test Facility
- WENO: Weighted essentially non-oscillatory